

# VEGF promotes diabetic retinopathy by upregulating the PKC/ET/NF- $\kappa$ B/ICAM-1 signaling pathway

Meiying Zhang, Min Zhou, Xia Cai, Yan Zhou, Xueling Jiang, Yan Luo, Yue Hu, Rong Qiu, Yanrong Wu, Yuejin Zhang, Yan Xiong

*Department of Endocrinology, the Second Affiliated Hospital of Nanchang University, Jiangxi, China*

## ABSTRACT

Diabetic retinopathy (DR) is a common microvascular complication in patients with diabetes mellitus. DR is caused by chronic hyperglycemia and characterized by progressive loss of vision because of damage to the retinal microvasculature. In this study, we investigated the regulatory role and clinical significance of the vascular endothelial growth factor (VEGF)/protein kinase C (PKC)/endothelin (ET)/nuclear factor- $\kappa$ B (NF- $\kappa$ B)/intercellular adhesion molecule 1 (ICAM-1) signaling pathway in DR using a rat model. Intraperitoneal injections of the VEGF agonist, streptozotocin (STZ) were used to generate the DR model rats. DR rats treated with the VEGF inhibitor (DR+VEGF inhibitor) were used to study the specific effects of VEGF on DR pathology and the underlying mechanisms. DR and DR+VEGF agonist rats were injected with the PKC $\beta$ 2 inhibitor, GF109203X to determine the therapeutic potential of blocking the VEGF/PKC/ET/NF- $\kappa$ B/ICAM-1 signaling pathway. The body weights and blood glucose levels of the rats in all groups were evaluated at 16 weeks. DR-related retinal histopathology was analyzed by hematoxylin and eosin staining. ELISA assay was used to estimate the PKC activity in the retinal tissues. Western blotting and RT-qPCR assays were used to analyze the expression levels of PKC- $\beta$ 2, VEGF, ETs, NF- $\kappa$ B, and ICAM-1 in the retinal tissues. Immunohistochemistry assay was used to analyze VEGF and ICAM-1 expression in the rat retinal tissues. Our results showed that VEGF, ICAM-1, PKC $\beta$ 2, ET, and NF- $\kappa$ B expression levels as well as PKC activity were significantly increased in the retinal tissues of the DR and DR+VEGF agonist rat groups compared to the control and DR+VEGF inhibitor rat groups. DR and DR+VEGF agonist rats showed significantly lower body weight and significantly higher retinal histopathology scores and blood glucose levels compared to the control and DR+VEGF inhibitor group rats. However, treatment of DR and DR+VEGF agonist rats with GF109203X partially alleviated DR pathology by inhibiting the VEGF/PKC/ET/NF- $\kappa$ B/ICAM-1 signaling pathway. In summary, our data demonstrated that inhibition of the VEGF/PKC/ET/NF- $\kappa$ B/ICAM-1 signaling pathway significantly alleviated DR-related pathology in the rat model. Therefore, VEGF/PKC/ET/NF- $\kappa$ B/ICAM-1 signaling axis is a promising therapeutic target for DR.

**Key words:** diabetic retinopathy; VEGF; ICAM-1; PKC/ET/NF- $\kappa$ B; streptozotocin.

**Correspondence:** Yan Xiong, Department of Endocrinology, The Second Affiliated Hospital of Nanchang University. No.1 Minde Road, Nanchang, Jiangxi 330006, China. E-mail: xiong6665662@163.com

**Contributions:** YX, conceived and designed the study; MYZ, performed the experiments and drafted the manuscript; MYZ, MZ, XC, performed the literature search and data analysis; YZ, XLJ, YL, assisted with the data analysis; YH, RQ, YRW, YJZ, compiled the discussion for the results; YX, MYZ, MZ, XC, revised the manuscript. All the authors reviewed the final manuscript, read and approved the final version of and agreed to be accountable for all aspects of the work.

**Funding:** This study was supported by the Key projects of Jiangxi Provincial Department of Science and Technology (Grant No. 20202BBGL73022).

**Availability of data and materials:** The data of this study is available from the corresponding author upon request.

**Ethics approval:** The experimental protocols in this study were approved by the Ethics Committee of the Second Affiliated Hospital of Nanchang University.

**Conflict of interest:** The authors declare that they have no competing interests, and all authors confirm accuracy.

## Introduction

Diabetic retinopathy (DR) is a common diabetes-related microvascular disease of the eye that causes progressive loss of vision or blindness, and is characterized by retinal edema, exudation, hemorrhage, neovascularization, and changes in the proliferative membrane.<sup>1,2</sup> In patients with DR, the chronic hyperglycemic environment induces expression and secretion of pro-inflammatory cytokines, which alter metabolic pathways and the blood-retinal barrier function, inhibit endothelial cell proliferation, and stimulate aberrant angiogenesis.<sup>3</sup>

DR is primarily treated with anti-platelet coagulation drugs, fibrinolytic enzymes, and intravitreal injections of vascular endothelial growth factor (VEGF) to suppress fundus edema and neovascularization.<sup>4</sup> Furthermore, some patients are surgically treated by retinal laser photocoagulation to improve vision by removing the surrounding neovascularization.<sup>5</sup> However, the light energy from the laser can also damage the outer layer of the retina and the nerve fibers around the optic disc, thereby aggravating visual field defects and visual impairment.<sup>6</sup> Hence, there is an urgent need to discover novel therapeutic targets for DR to improve treatment outcomes.

VEGF is a potent pro-angiogenic growth factor that is associated with the development of diabetes-related ophthalmopathy.<sup>7</sup> In the normal healthy eyes, low levels of VEGF are expressed and secreted by the peripheral retinal cells, endothelial cells, and the retinal pigment epithelial cells.<sup>8-10</sup> In patients with DR, retinal VEGF levels are significantly elevated and correlate with higher IGF-1 levels and insulin resistance.<sup>11,12</sup> However, specific molecular mechanisms regarding the regulation of DR progression by VEGF remain obscure.

VEGF and intercellular adhesion molecule 1 (ICAM-1) coordinately regulate aberrant retinal angiogenesis in patients with DR.<sup>13</sup> VEGF induces expression of ICAM-1 in the retina and initiates retinal leukocyte adhesion, which promotes early breakdown of the blood-retina barrier, capillary non-perfusion, and endothelial cell damage and death.<sup>14</sup> Furthermore, ICAM-1 expression is induced by the activation of the PKC/ET/NF- $\kappa$ B signaling pathway.<sup>15-17</sup> However, the specific role of the VEGF/PKC/ET/NF- $\kappa$ B/ICAM-1 signaling axis in DR progression has not been described.

Therefore, in this study, we investigated the regulatory role of the VEGF/PKC/ET/NF- $\kappa$ B/ICAM-1 signaling axis in the onset and progression of DR using a rat model.

## Materials and Methods

### Establishment of DR *in vivo* model

The animal experimental protocols were performed as approved by the Animal Ethics committee of the Second Affiliated Hospital of Nanchang University, Jiangxi, China. We purchased healthy, distantly related, 1-month-old SPF-grade male SD rats weighing 220 $\pm$ 20 g from the Experimental Animal Center of the Second Affiliated Hospital of Nanchang University. They were housed in the SPF grade Experimental Animal Center under laboratory conditions in accordance with the recommendations from the Administration of Laboratory Animals of the State Science and Technology Commission and the code of ethics for animals. The rats were randomly divided into six experimental groups, namely, NC, DR, DR + VEGF inhibitor, DR + VEGF agonist, DR + GF109203X, and DR + VEGF agonist + GF109203X groups.

The SD rats were acclimatized for 5 days and were fed with

normal chow with free access to water. For the DR treatment, 10 g/L streptozotocin (STZ) was dissolved in 0.1 mol/L citrate buffer (pH = 4.5) and injected intraperitoneally at a dose of 60 mg/kg. The NC group and DR rats were administered intravitreal injections with 10  $\mu$ L of 1% dimethyl sulfoxide, whereas the GF109203X group was administered 10  $\mu$ L of GF109203X at a concentration of 10<sup>-5</sup> mol/L in 1% DMSO.

### Estimation of blood glucose levels in rats

The rats were fasted for 72 h and briefly anesthetized with ether. The blood samples were collected from the caudal vein and centrifuged at 3000 rpm for 10 min. The serum samples were stored in a refrigerator at -20°C until further use. The blood glucose levels were measured in the BK-500 automatic biochemical analyzer (Biobase Biotech Ltd., Jinan city, China). The blood glucose levels in diabetic rats were higher than 16.7 mmol/L.

### Immunohistochemistry staining

The enucleated eyeballs of rats were harvested, fixed in 4% paraformaldehyde, paraffin embedded, and sectioned into 4- $\mu$ m-thick slices. The fixed, paraffin-embedded sections were dewaxed and hydrated by incubating the slices in xylene, followed by incubation in different concentrations of solutions with serially diluted concentrations of alcohol. The tissue slices were incubated in citrate buffer with Triton X-100. Then, antigen retrieval was performed by incubating the tissue sections in a 95°C water bath for 15 min followed by cooling to room temperature. Then, after rinsing and blocking at room temperature, the sections were incubated overnight at 4°C with primary antibodies against VEGF (1:350; Cat. No. ab1316, Abcam, Cambridge, UK) and ICAM-1 (1:600; Cat. No. ab282575, Abcam). The samples were then incubated for 40 min at 37°C with the HRP-conjugated rabbit anti-Rat IgG (H&L) secondary antibody (1:500; Cat. No. ab6734 Abcam). Then, color development was performed with DAB. The sections were counter-stained with hematoxylin and analyzed using the Motic high-resolution color image measurement system. Brown granular staining was considered as a positive signal.

### Western blotting

The whole protein extracts of retinal tissues were prepared by incubation with the RIPA lysis buffer (AS1004, ASPEN, Wuhan, China). The total protein content of the samples was analyzed using the BCA assay. Equal amounts of protein extracts were separated by SDS-PAGE and transferred onto PVDF membranes. The membranes were blocked with 5% skimmed milk for 2 h at room temperature. Then, the blots were incubated overnight at 4°C with primary antibodies such as anti-VEGF (1:500; cat. no. ab69479, Abcam), anti-ICAM-1 (1:600; Cat. No. ab282575, Abcam), anti-PKC $\beta$ 2 (1:1000; Cat. No. ab108970, Abcam), and anti- $\beta$ -actin (1:1000; Cat. No. ab8226, Abcam). The membranes were rinsed and then incubated at room temperature for 2 h with the HRP-conjugated rabbit anti-mouse IgG H&L secondary antibody (1:2000; Abcam, Cat. No. ab6728). The blots were developed using the ECL reagent (AS1059, ASPEN). The grayscale values of the protein bands were analyzed by the Image-Pro Plus system. The relative expression of the proteins was analyzed using  $\beta$ -actin as the internal reference control.

### Hematoxylin and Eosin (H&E) staining

The retinal tissues of rats were fixed in 4% paraformaldehyde solution for 24 h. The fixed retinal tissues were dehydrated in gradient alcohol solutions, waxed, and paraffin embedded. Then, 4- $\mu$ m-thick retinal tissue sections were cut, dewaxed with xylene, and hydrated with gradient alcohol solutions. The sections were stained by first incubating with the hematoxylin solution for 10

min followed by the eosin solution for 10 min. The stained sections were dehydrated again with gradient alcohol, sealed with neutral gum, and photographed under a light microscope.

### RT-qPCR analysis

Retinal tissues were extracted from the enucleated eyeballs of rats and frozen at  $-80^{\circ}\text{C}$ . Total RNA was extracted from the retinal tissue samples using the TRIpure Total RNA Extraction Reagent (EP013, ELK Biotechnology Co. Ltd., Wuhan, China) and quantified by estimating the absorbance values (OD) at 260 nm and 280 nm. The quality of RNA samples was determined using the OD260/OD280 ratio and samples with values between 1.8 and 2.0 were used for further analysis. The cDNA was synthesized from the total RNA samples using the M-MLV Reverse Transcriptase Reagent (EQ002, ELK Biotechnology). The cDNA samples were used as a template and amplified using StepOne™ Real-Time PCR System (Life Technologies, Carlsbad, CA, USA). The qPCR cycling conditions included initial denaturation at  $95^{\circ}\text{C}$  for 3 min followed by 45 cycles at  $95^{\circ}\text{C}$  for 10 s,  $58^{\circ}\text{C}$  for 45 s, and  $72^{\circ}\text{C}$  for 29 s. The relative gene expression were analyzed using the  $2^{-\Delta\Delta\text{CT}}$  method using  $\beta$ -actin as the internal reference.

### ELISA assay

The cytoplasmic and membrane protein samples were prepared from the retinal tissues, which were isolated from the nuclei-free eyeballs of rats. PKC Kinase activity was analyzed using the PKC Kinase Activity Assay Kit (ab139437; Abcam) according to the manufacturer's instructions. The protein concentration of the sam-

ples and the absorbance (OD at 450 nm) values for the PKC kinase activity were determined using the DR-200Bs microplate reader (Diatek, Wuxi, China). PKC activity = OD/(protein content  $\times$  reaction time).

### Statistical analysis

Statistical analysis was performed using the SPSS 19.0 software (IBM Corp., Armonk, NY, USA). The data were expressed as means  $\pm$  standard deviation (SD). One-way ANOVA followed by Tukey's *post-hoc* test was used to compare the statistical differences between multiple experimental groups.  $P < 0.05$  was considered as statistically significant.

## Results

### VEGF inhibition improves body weight, decreased histopathological characteristics of the retinal tissues and normalizes blood glucose levels in the DR rats

The rats of DR group showed significantly lower body weight and significantly higher blood glucose levels compared to the NC group rats at 16 weeks (Figure 1 A,C). H&E staining results demonstrated that the inner nuclear layer (INL), outer nuclear layer (ONL), and the cell density in the ganglion cell layer of the retinal tissues were significantly reduced in the DR group rats compared to the NC group rats (Figure 1B). These results demonstrated successful establishment of the DR model rats.

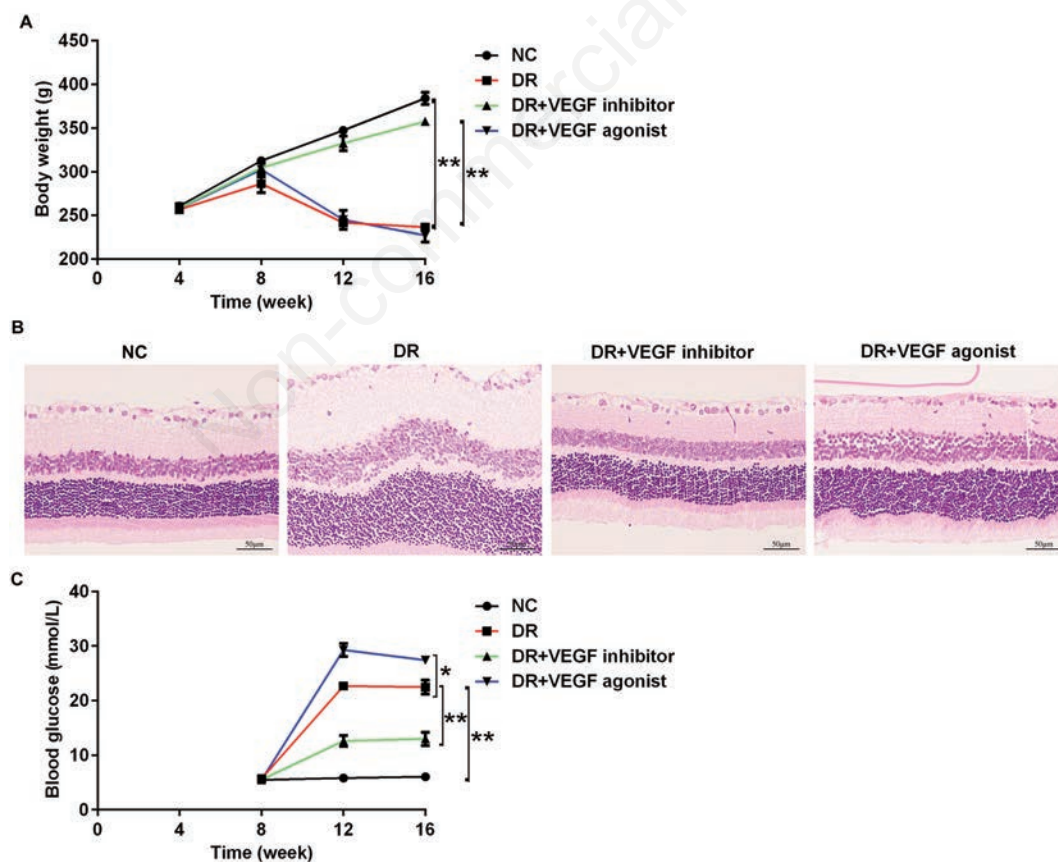


**Figure 1.** Effects of the VEGF agonist and VEGF inhibitor on the DR pathology in rats. A) Body weights of the NC, DR, DR + VEGF inhibitor, and DR + VEGF agonist group rats at 16 weeks. B) H&E staining results demonstrate the histopathological characteristics of the retinal tissues from the NC, DR, DR + VEGF inhibitor, and DR + VEGF agonist group rats. C) Blood glucose levels in the NC, DR, DR + VEGF inhibitor, and DR + VEGF agonist group rats at 16 weeks. \* $p < 0.05$ ; \*\* $p < 0.01$ .

After confirming the successful generation of the DR model rats, the DR group rats were further divided into DR+VEGF inhibitor and DR+VEGF agonist groups to determine the effects of VEGF inhibition or VEGF overexpression on DR pathology. The DR model rats treated with STZ (VEGF inhibitor) showed increased body weight, lower blood glucose levels, and amelioration of the DR-related histopathological features in the retinal tissues compared with the DR group rats (Figure 1 A-C). On the contrary, DR model rats treated with the VEGF agonist showed reduced body weight, increased blood glucose levels, and further exacerbation of the DR-related histopathological features in the retinal tissues compared to the DR group rats (Figure 1 A-C).

### VEGF regulates ICAM-1 expression in the retinal tissues of the DR model rats

The retinal tissues of the DR group rats showed significantly higher VEGF and ICAM-1 mRNA and protein levels compared to the NC group rats (Figure 2 A-D). Furthermore, VEGF and ICAM-1 expression levels in the retinal tissues were significantly reduced in the DR + VEGF inhibitor group and significantly increased in the DR + VEGF agonist group compared with the DR group (Figure 2 A-D). This suggested that VEGF regulated ICAM-1 expression levels in the retinal tissues of the DR group rats.

### VEGF regulates DR progression *via* the PKC/ET/NF- $\kappa$ B/ICAM-1 signaling pathway

Next, we analyzed if VEGF regulated DR progression *via* the PKC/ET/NF- $\kappa$ B signaling pathway. ELISA, Western blotting and RT-qPCR assays showed that PKC activity and the expression lev-

els of PKC $\beta$ 2, ET-1, ET-3, ET-A, ET-B, and NF- $\kappa$ B were significantly higher in the retinal tissues of the DR group rats compared to the NC group rats (Figure 3 A-H). Furthermore, PKC activity and the PKC $\beta$ 2, ET-1, ET-3, ET-A, ET-B, and NF- $\kappa$ B mRNA and protein expression levels were significantly reduced in the retinal tissues of the DR + VEGF inhibitor group rats and significantly increased in the retinal tissues of the DR + VEGF agonist group rats compared to the DR rats (Figure 3 A-H). These results suggested that VEGF promoted DR by activating the PKC/ET/NF- $\kappa$ B/ICAM-1 signaling pathway.

### PKC $\beta$ 2 inhibitor reduces DR progression by suppressing VEGF-induced activation of the PKC/ET/NF- $\kappa$ B/ICAM-1 signaling pathway

Next, we treated DR rats with GF109203X, a PKC $\beta$ 2 inhibitor, to confirm the regulatory role of the PKC signaling pathway in DR pathology. The rats were divided into the DR, DR + VEGF agonist, DR + GF109203X, and DR + VEGF agonist + GF109203X groups. The body weights of rats were lowest in the DR + VEGF agonist group and highest in the DR + GF109203X group after 16 weeks of treatment (Figure 4A). Furthermore, body weights of rats in the DR + VEGF agonist + GF109203X group were higher than the rats in the DR + VEGF agonist group (Figure 4A). Moreover, in comparison with the DR group, blood glucose levels, PKC activity, and the DR-related histopathological features were significantly decreased in the DR + GF109203X group and significantly increased in the DR + VEGF agonist group (Figure 4 B-E). Besides, VEGF agonist-related augmentation of the DR histopathological features and blood glucose levels were partially

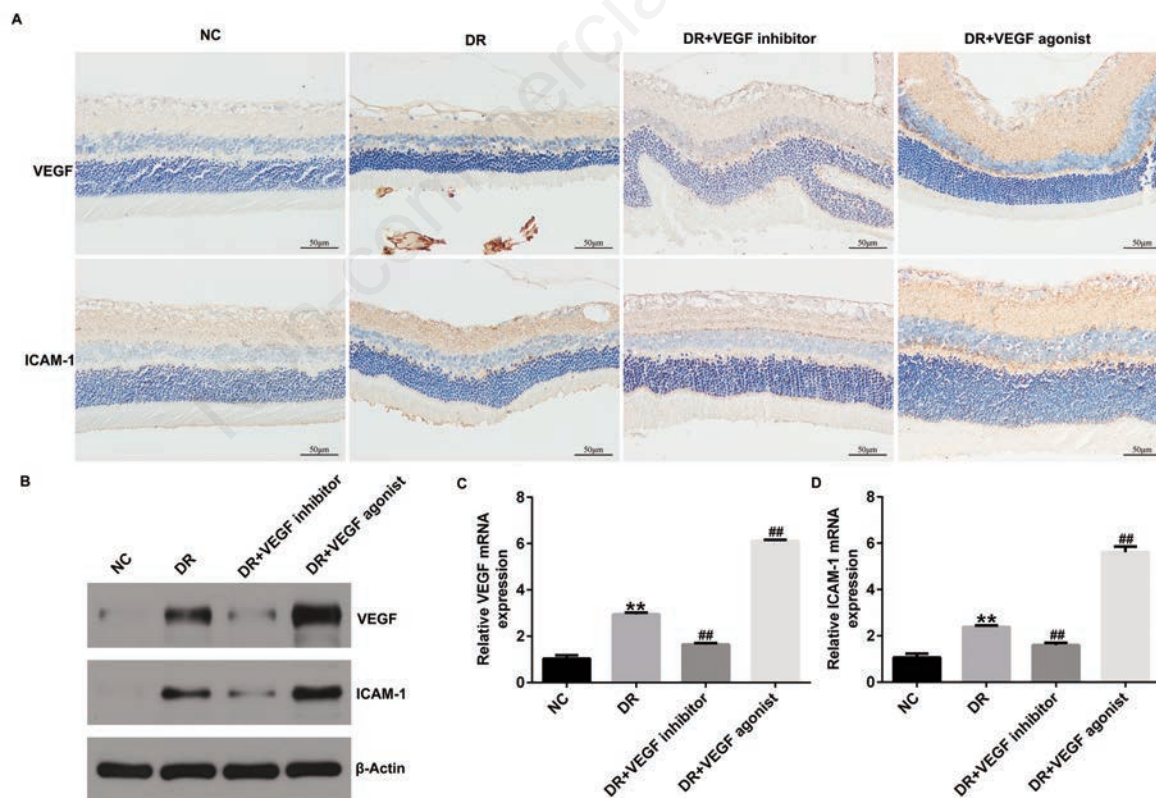


**Figure 2.** VEGF regulates ICAM-1 expression in the retinal tissues of the DR model rats. A) Immunohistochemistry results show the VEGF and ICAM-1 protein expression levels in the retinal tissues of the NC, DR, DR + VEGF inhibitor, and DR + VEGF agonist group rats. B) Western blot results show the VEGF and ICAM-1 protein levels in the retinal tissues of the NC, DR, DR + VEGF inhibitor, and DR + VEGF agonist group rats (C,D) RT-qPCR results show the VEGF and ICAM-1 mRNA levels in the retinal tissues of the NC, DR, DR + VEGF inhibitor, and DR + VEGF agonist group rats. \*\* $p < 0.01$  vs NC; ## $p < 0.01$  vs DR.

reduced in the DR+VEGF agonist+GF109203X group rats (Figure 4 B,C). PKC activity was significantly reduced in the retinal tissues of the DR+VEGF agonist+GF109203X group rats compared to the DR+VEGF agonist group (Figure 4 D,E).

The expression levels of VEGF, ICAM-1, ETs, and NF- $\kappa$ B were highest in the retinal tissues of the DR+VEGF agonist group rats and lowest in the retinal tissues of the DR+GF109203X group rats (Figures 5 and 6). Furthermore,

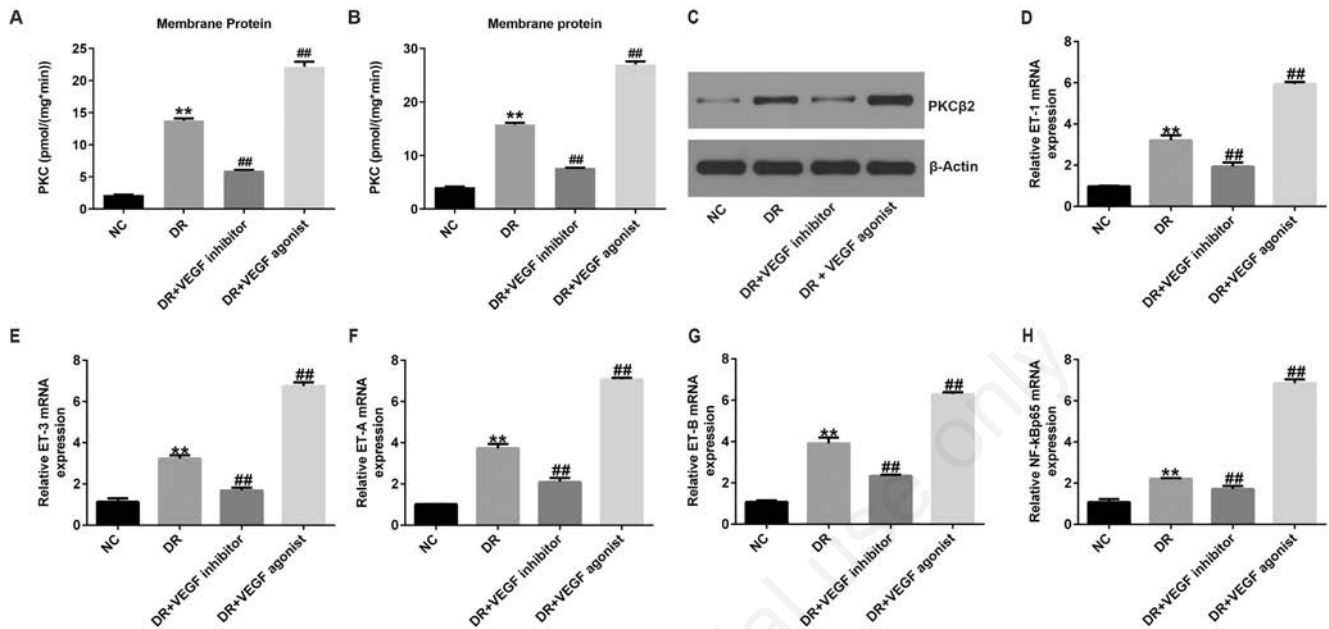


**Figure 3.** VEGF regulates PKC activity and the PKC/ET/NF- $\kappa$ B signaling pathway in the retinal tissues of the DR model rats. A,B) ELISA assay results show the (A) membrane and (B) cytoplasmic PKC activity in the retinal tissues of the NC, DR, DR+VEGF inhibitor, and DR+VEGF agonist group rats. C) Western blotting analysis shows the expression levels of PKC $\beta$ 2 in the retinal tissues of the NC, DR, DR + VEGF inhibitor, and DR + VEGF agonist group rats. D-H) RT-qPCR analysis shows the mRNA expression levels of ET-1 (D), ET-3 (E), ET-A (F), ET-B (G), and NF- $\kappa$ B (H) in the retinal tissues of the NC, DR, DR + VEGF inhibitor, and DR + VEGF agonist group rats. \*\* $p < 0.01$  vs NC; ## $p < 0.01$  vs DR.

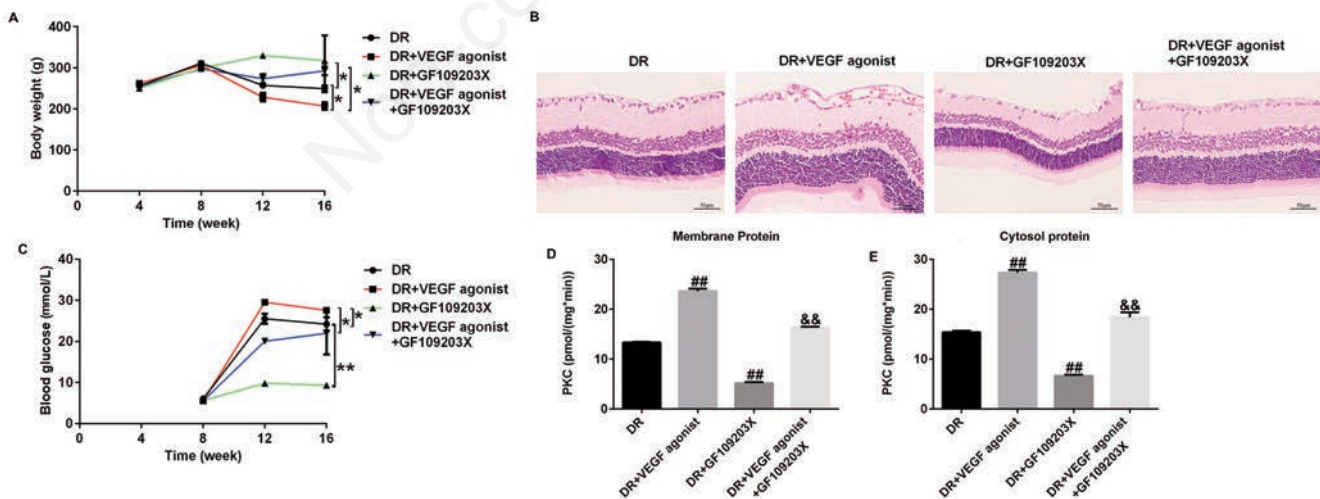


**Figure 4.** PKC $\beta$ 2 inhibitor suppresses VEGF-induced PKC activity and related pathology in the retinal tissues of the DR rats. A) Bar plot shows the body weight of the NC, DR, DR+VEGF agonist, DR+GF109203X, and DR+VEGF agonist+GF109203X group rats at 16 weeks after the beginning of treatment. B) H&E staining data shows the morphological changes in the retinal tissues of the NC, DR, DR+VEGF agonist, DR+GF109203X, and DR+VEGF agonist+GF109203X group rats. C) Blood glucose levels in the NC, DR, DR+VEGF agonist, DR+GF109203X, and DR+VEGF agonist+GF109203X group rats. D,E) ELISA assay results show the membrane and cytosolic PKC activity in the retinal tissues of the NC, DR, DR+VEGF agonist, DR+GF109203X, and DR+VEGF agonist+GF109203X group rats. \* $p < 0.05$ ; \*\* $p < 0.01$ ; ## $p < 0.01$  vs DR; && $p < 0.01$  vs DR+VEGF agonist.

VEGF agonist-induced hyperactivation of the PKC/ET/NF- $\kappa$ B/ICAM-1 signaling axis in the retinal tissues of the DR rats was reversed by treatment with GF109203X (Figures 5 and 6).

These data demonstrated that GF109203X suppressed VEGF-induced DR progression by inhibiting the PKC/ET/NF- $\kappa$ B/ICAM-1 signaling pathway.

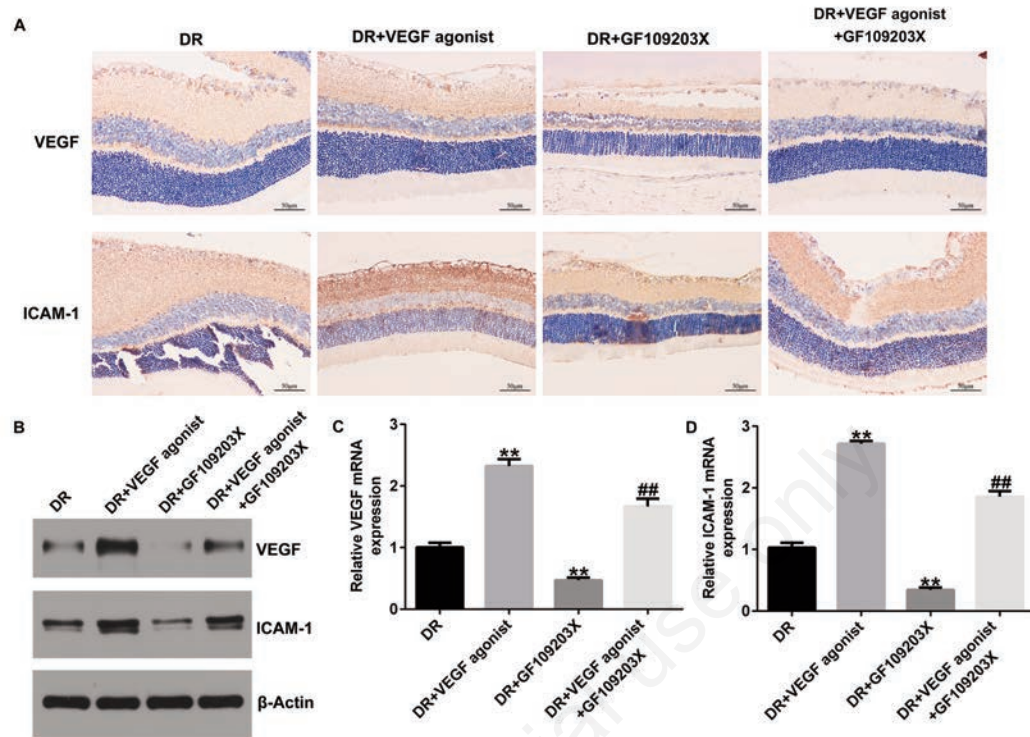


**Figure 5.** PKC $\beta$ 2 inhibitor decreases VEGF and ICAM-1 expression levels in the retinal tissues of the DR rats. A) Immunohistochemistry analysis shows the expression levels of VEGF and ICAM-1 proteins in the retinal tissues of the NC, DR, DR+VEGF agonist, DR+GF109203X, and DR+VEGF agonist+GF109203X group rats. B) Western blotting analysis shows the expression levels of VEGF and ICAM-1 proteins in the retinal tissues of the NC, DR, DR+VEGF agonist, DR+GF109203X, and DR+VEGF agonist+GF109203X group rats. C) RT-qPCR results show the VEGF and ICAM-1 mRNA levels in the retinal tissues of the NC, DR, DR+VEGF agonist, DR+GF109203X, and DR+VEGF agonist+GF109203X group rats. \*\* $p < 0.01$  vs DR; ## $p < 0.01$  vs DR+VEGF agonist.

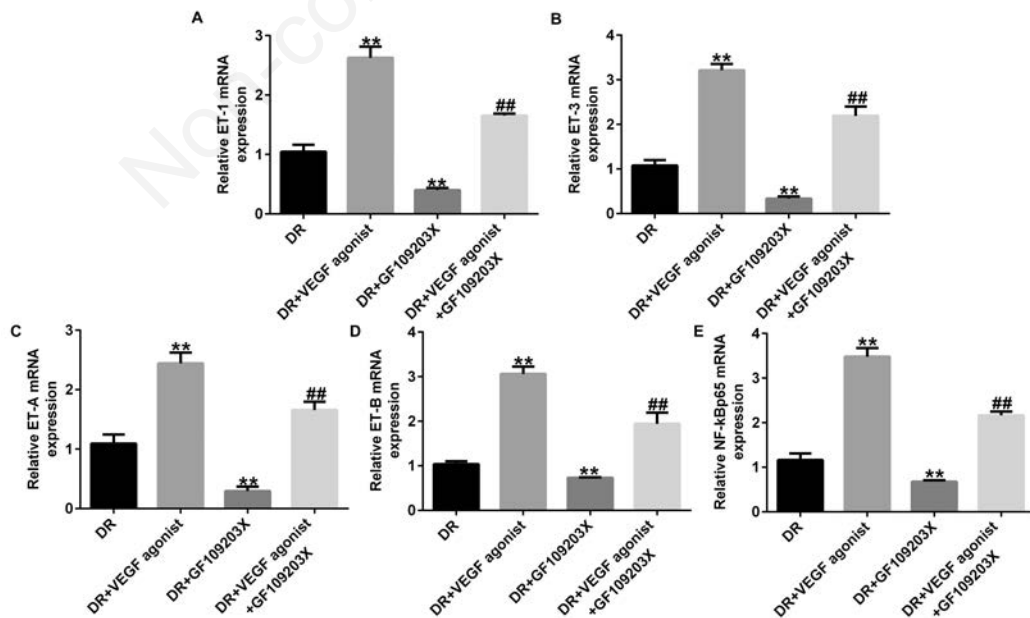


**Figure 6.** PKC $\beta$ 2 inhibitor inhibits transcription of ETs and NF- $\kappa$ B in the retinal tissues of the DR model rats. A-E) RT-qPCR analysis show the mRNA expression levels of ET-1 (A), ET-3 (B), ET-A (C), ET-B (D), and NF- $\kappa$ B (E) in the retinal tissues of the NC, DR, DR+VEGF agonist, DR+GF109203X, and DR+VEGF agonist+GF109203X group rats. \*\* $p < 0.01$  vs DR; ## $p < 0.01$  vs DR+VEGF agonist.

## Discussion

VEGF is one of the main mediators of DR because it stimulates vascular endothelial cell growth and proliferation, and neovascularization in the retinal tissues.<sup>8,18</sup> In the normal physiological state, low expression of VEGF is required to maintain and repair vascular damage in the various tissues of the human body.<sup>8-10</sup> However, in the diabetic patients, hyperglycemia and dyslipidemia induces an hypoxic environment, which stimulates VEGF overexpression and secretion.<sup>19</sup> In our study, treatment of rats with STZ (VEGF agonist) increased the expression levels of VEGF and were accompanied with decreased body weight and increased blood glucose levels and histopathological scores. This demonstrated successful generation of the *in vivo* DR model rats.

PKC represents a family of phospholipid-dependent serine/threonine protein kinases with several isoforms that are widely found in most cells and tissues including the retina, kidney, and heart.<sup>20</sup> PKC activation is associated with cellular proliferation, differentiation, and apoptosis.<sup>21,22</sup> Chronic hyperglycemia induces hypoxia, which in turn promotes neovascularization by activating PKC.<sup>23,24</sup> Several studies have shown that activation of PKC plays a crucial role in DR pathology. For example, Choi *et al.* and Sarikaya *et al.* reported elevated PKC activity in the *in vitro* and *in vivo* DR models.<sup>25,26</sup> The expression of PKC $\beta$ 2, a subtype of PKC, is associated with obesity and related metabolic diseases.<sup>27,28</sup> Furthermore, activation of PKC promotes overexpression of endothelins (ETs), which are potent vasoconstrictors that adversely affect the endothelial function of the blood vessels and cause retinal damage.<sup>29-31</sup> NF- $\kappa$ B is a ubiquitous transcription factor that regulates gene expression in response to stimulation by cytokines and other growth and inflammatory factors.<sup>32</sup> Recent studies have shown that NF- $\kappa$ B is closely associated with the onset and progression of diabetic vascular lesions.<sup>33,34</sup> Furthermore, the expression of NF- $\kappa$ B is significantly increased in response to a long-term high-glucose environment.<sup>35,36</sup> Therefore, NF- $\kappa$ B plays an essential role in the onset and progression of DR. Consistent with previous studies, our data demonstrated elevated PKC activity and activation of the PKC/ET/NF- $\kappa$ B signaling pathway in the STZ-triggered DR rats. Furthermore, treatment of DR rats with the VEGF agonist resulted in hyper-activation of the PKC/ET/NF- $\kappa$ B signaling pathway, whereas, treatment with the VEGF inhibitor significantly decreased activation of the PKC/ET/NF- $\kappa$ B pathway.

ICAM-1 is a cell surface glycoprotein and a key player in inflammatory responses and immune regulation.<sup>37</sup> ICAM-1 is an essential member of the ICAM family that participates in signaling pathways that mediate secretion of various inflammatory factors, stimulate the attachment of leukocytes to the capillary endothelium, and induce vascular endothelial injury.<sup>38,39</sup> Therefore, suppression of ICAM-1 gene expression alleviates infiltration of inflammatory cells and reduces microvascular injury. ICAM-1 expression is significantly up-regulated in patients with DR.<sup>40,41</sup> Our data also demonstrated elevated expression of ICAM-1 in the STZ-induced DR rats. Furthermore, our study demonstrated that the VEGF agonist significantly increased ICAM-1 expression through the PKC/ET/NF- $\kappa$ B signaling pathway and aggravated DR.

Our study has few limitations. We did not investigate if the expression levels of ICAM-1 modulated the expression levels of VEGF in DR. Moreover, further studies are necessary to identify the downstream targets of ICAM-1 and VEGF in DR.

In conclusion, our study demonstrated that VEGF increased ICAM-1 expression through the PKC/ET/NF- $\kappa$ B signaling pathway in DR. Furthermore, VEGF inhibitor and the PKC inhibitor significantly reduced DR pathology by suppressing the VEGF/PKC/ET/NF- $\kappa$ B/ICAM-1 signaling activity. Therefore, VEGF/PKC/ET/NF- $\kappa$ B/ICAM-1 signaling pathway is a potential therapeutic target for DR.

## References

- Wang W, Lo ACY. Diabetic retinopathy: Pathophysiology and treatments. *Int J Mol Sci* 2018;19:1816.
- Noor-UI-Huda M, Tehsin S, Ahmed S, Niazi FAK, Murtaza Z. Retinal images benchmark for the detection of diabetic retinopathy and clinically significant macular edema (CSME). *Biomed Tech (Berl)* 2019;64:297-307.
- Tang L, Zhang C, Yang Q, Xie H, Liu D, Tian H, et al. Melatonin maintains inner blood-retinal barrier via inhibition of p38/TXNIP/NF-kappaB pathway in diabetic retinopathy. *J Cell Physiol* 2021;236:5848-64.
- Singh SR, Parameswarappa DC, Govindahari V, Lupidi M, Chhablani J. Clinical and angiographic characterization of choroidal neovascularization in diabetic retinopathy. *Eur J Ophthalmol* 2021;31:584-91.
- Ohlhausen M, Payne C, Greenlee T, Chen AX, Conti T, Singh RP. Impact and characterization of delayed pan-retinal photocoagulation in proliferative diabetic retinopathy. *Am J Ophthalmol* 2021;223:267-74.
- Wadhvani M, Bhartiya S, Upadhaya A, Manika M. A meta-analysis to study the effect of pan retinal photocoagulation on retinal nerve fiber layer thickness in diabetic retinopathy patients. *Rom J Ophthalmol* 2020;64:8-14.
- Kim EJ, Lin WV, Rodriguez SM, Chen A, Loya A, Weng CY. Treatment of diabetic macular edema. *Curr Diab Rep* 2019;19:68.
- Cheng J, Yang HL, Gu CJ, Liu YK, Shao J, Zhu R, et al. Melatonin restricts the viability and angiogenesis of vascular endothelial cells by suppressing HIF-1alpha/ROS/VEGF. *Int J Mol Med* 2019;43:945-55.
- Sant DW, Camarena V, Mustafi S, Li Y, Wilkes Z, Van Booven D, et al. Ascorbate suppresses VEGF Expression in retinal pigment epithelial cells. *Invest Ophthalmol Vis Sci* 2018;59:3608-18.
- Simmons AB, Bretz CA, Wang H, Kunz E, Hajj K, Kennedy C, et al. Gene therapy knockdown of VEGFR2 in retinal endothelial cells to treat retinopathy. *Angiogenesis* 2018;21:751-64.
- El-Sehrawy AA, Elkhamisy EM, Badawi AE, Elshahawy HA, Elsayed E, Mohammed NT, et al. Subclinical hypothyroidism in patients with diabetic retinopathy: Role of vascular endothelial growth factor. *Endocr Metab Immune Disord Drug Targets* 2022;22:502-9.
- Wang H, Lou H, Li Y, Ji F, Chen W, Lu Q, et al. Elevated vitreous Lipocalin-2 levels of patients with proliferative diabetic retinopathy. *BMC Ophthalmol* 2020;20:260.
- Zhou KK, Benyajati S, Le Y, Cheng R, Zhang W, Ma JX. Interruption of Wnt signaling in Muller cells ameliorates ischemia-induced retinal neovascularization. *PLoS One* 2014;9:e108454.
- Jain A, Saxena S, Khanna VK, Shukla RK, Meyer CH. Status of serum VEGF and ICAM-1 and its association with external limiting membrane and inner segment-outer segment junction disruption in type 2 diabetes mellitus. *Mol Vis* 2013;19:1760-8.
- Lee AS, Kim JS, Lee YJ, Kang DG, Lee HS. Anti-TNF-alpha activity of *Portulaca oleracea* in vascular endothelial cells. *Int J Mol Sci* 2012;3:5628-44.
- Xia J, Ozaki I, Matsuhashi S, Kuwashiro T, Takahashi H, Anzai K, et al. Mechanisms of PKC-mediated enhancement of HIF-1alpha activity and its inhibition by vitamin K2 in hepatocellular carcinoma cells. *Int J Mol Sci* 2019;20:1022.
- Zaidi N, Quezada SA, Kuroiwa JMY, Zhang L, Jaffee EM, Steinman RM, et al. Anti-CTLA-4 synergizes with dendritic cell-targeted vaccine to promote IL-3-dependent CD4(+) effector T cell infiltration into murine pancreatic tumors. *Ann N Y Acad Sci* 2019;1445:62-73.

18. Arrigo A, Aragona E, Bandello F. VEGF-targeting drugs for the treatment of retinal neovascularization in diabetic retinopathy. *Ann Med* 2022;54:1089-111.
19. Yin Z, Tan R, Yuan T, Chen S, Quan Y, Hao Q, et al. Berberine prevents diabetic retinopathy through inhibiting HIF-1 $\alpha$ /VEGF/ NF-kappa B pathway in db/db mice. *Pharmazie* 2021;76:165-71.
20. Wu QW, Kapfhammer JP. Serine/threonine kinase 17b (STK17B) signalling regulates Purkinje cell dendritic development and is altered in multiple spinocerebellar ataxias. *Eur J Neurosci* 2021;54:6673-84.
21. Nadel G, Yao Z, Ben-Ami I, Naor Z, Seger R. Gq-induced apoptosis is mediated by AKT inhibition that leads to PKC-induced JNK activation. *Cell Physiol Biochem* 2018;50:121-35.
22. Wang X, Ge Y, Shi M, Dai H, Liu W, Wang P. Protein kinase N1 promotes proliferation and invasion of liver cancer. *Exp Ther Med* 2021;21:651.
23. Huang D, Wang FB, Guo M, Li S, Yan ML, Yu T, et al. Effect of combined treatment with rosuvastatin and protein kinase Cbeta2 inhibitor on angiogenesis following myocardial infarction in diabetic rats. *Int J Mol Med* 2015;35:829-38.
24. Moriya J, Ferrara N. Inhibition of protein kinase C enhances angiogenesis induced by platelet-derived growth factor C in hyperglycemic endothelial cells. *Cardiovasc Diabetol* 2015;14:19.
25. Choi JA, Chung YR, Byun HR, Park H, Koh JY, Yoon YH. The anti-ALS drug riluzole attenuates pericyte loss in the diabetic retinopathy of streptozotocin-treated mice. *Toxicol Appl Pharmacol* 2017;315:80-9.
26. Sarikaya M, Yazihan N, Das Evcimen N. Relationship between aldose reductase enzyme and the signaling pathway of protein kinase C in an in vitro diabetic retinopathy model. *Can J Physiol Pharmacol* 2020;98:243-51.
27. Shu Y, Hassan F, Coppola V, Baskin KK, Han X, Mehta NK, et al. Hepatocyte-specific PKCbeta deficiency protects against high-fat diet-induced nonalcoholic hepatic steatosis. *Mol Metab* 2021;44:101133.
28. Tai H, Wang X, Zhou J, Han X, Fang T, Gong H, et al. Protein kinase Cbeta activates fat mass and obesity-associated protein by influencing its ubiquitin/proteasome degradation. *FASEB J* 2017;31:4396-406.
29. Chen YL, Ren Y, Rosa RH Jr., Kuo L, Hein TW. Contributions of sodium-hydrogen exchanger 1 and mitogen-activated protein kinases to enhanced retinal venular constriction to endothelin-1 in diabetes. *Diabetes* 2021;70:2353-63.
30. Zhai X, Leo MD, Jaggar JH. Endothelin-1 stimulates vasoconstriction through Rab11A serine 177 phosphorylation. *Circ Res* 2017;121:650-61.
31. Zhu Q, Xu X, Xia X, Gu Q, Ho PC. Role of protein kinase C on the alteration of retinal endothelin-1 in streptozotocin-induced diabetic rats. *Exp Eye Res* 2005;81:200-6.
32. Hou J, Jiang S, Zhao J, Zhu D, Zhao X, Cai JC, et al. N-Myc-interacting protein negatively regulates TNF-alpha-induced NF-kappaB transcriptional activity by sequestering NF-kappaB/p65 in the cytoplasm. *Sci Rep* 2017;7:14579.
33. Atic R, Devenci E. Endothelin 1, NF-kappaB, and ADAM-15 expression in diabetic foot wounds. *Bratisl Lek Listy* 2019;120:58-64.
34. Roy H, Bhardwaj S, Babu M, Kokina I, Uotila S, Ahtialansaari T, et al. VEGF-A, VEGF-D, VEGF receptor-1, VEGF receptor-2, NF-kappaB, and RAGE in atherosclerotic lesions of diabetic Watanabe heritable hyperlipidemic rabbits. *FASEB J* 2006 20:2159-61.
35. Liang WJ, Yang HW, Liu HN, Qian W, Chen XL. HMGB1 upregulates NF-kB by inhibiting IKB-alpha and associates with diabetic retinopathy. *Life Sci* 2020;241:117146.
36. Zhang T, Ouyang H, Mei X, Lu B, Yu Z, Chen K, et al. Erianin alleviates diabetic retinopathy by reducing retinal inflammation initiated by microglial cells via inhibiting hyperglycemia-mediated ERK1/2-NF-kappaB signaling pathway. *FASEB J* 2019;33:11776-90.
37. Bui TM, Wiesolek HL, Sumagin R. ICAM-1: A master regulator of cellular responses in inflammation, injury resolution, and tumorigenesis. *J Leukoc Biol* 2020;108:787-99.
38. Vitoria WO, Thome LS, Kanashiro-Galo L, Carvalho LV, Penny R, Santos WLC, et al. Upregulation of intercellular adhesion molecule-1 and vascular cell adhesion molecule-1 in renal tissue in severe dengue in humans: Effects on endothelial activation/dysfunction. *Rev Soc Bras Med Trop* 2019;52:e20180353.
39. Wang YQ, Song JJ, Han X, Liu YY, Wang XH, Li ZM, et al. Effects of angiopoietin-1 on inflammatory injury in endothelial progenitor cells and blood vessels. *Curr Gene Ther* 2014;14:128-35.
40. Turan M, Turan G. Immunoreactivity of ICAM-1, MMP-2, and Nesfatin-1 in lens epithelial cells of patients with diabetes mellitus with or without diabetic retinopathy. *Eur J Ophthalmol* 2022;32:255-62.
41. Yao Y, Du J, Li R, Zhao L, Luo N, Zhai JY, et al. Association between ICAM-1 level and diabetic retinopathy: a review and meta-analysis. *Postgrad Med J* 2019;95:162-8.

Received for publication: 10 August 2022. Accepted for publication: 29 September 2022.

This work is licensed under a Creative Commons Attribution-NonCommercial 4.0 International License (CC BY-NC 4.0).

©Copyright: the Author(s), 2022

Licensee PAGEPress, Italy

*European Journal of Histochemistry* 2022; 66:3522

doi:10.4081/ejh.2022.3522

*Publisher's note: All claims expressed in this article are solely those of the authors and do not necessarily represent those of their affiliated organizations, or those of the publisher, the editors and the reviewers. Any product that may be evaluated in this article or claim that may be made by its manufacturer is not guaranteed or endorsed by the publisher.*